

## Supplementary information for:

# Upcycling waste photovoltaic cells into silicon carbide via flash Joule heating

Ximing Zhang,<sup>a</sup> Feihong Guo,<sup>\*a</sup> Xiaoxiang Jiang,<sup>\*a</sup> Abdullah Hassan Hamadamin,<sup>b</sup> Adam. F. Lee,<sup>c</sup> Karen Wilson,<sup>c</sup> and Jabbar Gardy,<sup>d,e</sup>

<sup>a</sup>Engineering Laboratory for Energy System Process Conversion and Emission Control Technology of Jiangsu Province, School of Energy and Mechanical Engineering, Nanjing Normal University, Nanjing, 210042, China

<sup>b</sup>Department of Pharmaceutical Chemistry, Pharmacy College, Hawler Medical University, 44001, Erbil, Kurdistan Region, Iraq.

<sup>c</sup>Centre for Catalysis and Clean Energy, Griffith University, Gold Coast, QLD 4222, Australia

<sup>d</sup>School of Chemical and Process Engineering, University of Leeds, LS2 7QB, Leeds, United Kingdom

<sup>e</sup>Chemistry Department, College of Science, Salahaddin University-Erbil, 44002, Erbil, Iraqi Kurdistan Region

\*Corresponding author: fhguo@njnu.edu.cn (F. Guo); 62081@njnu.edu.cn (X. Jiang)

### Text S1. Material characterization

The crystalline phase and composition of materials was determined using a Rigaku-Ultima IV X-ray diffractometer equipped with Cu K $\alpha$  radiation ( $\lambda=1.5406$  Å), spanning  $2\theta = 5-90^\circ$ . Fourier transform infrared spectra were recorded using a Thermo Fisher Scientific Nicolet iS20 spectrometer. Raman spectra were recorded using a Horiba LabRAM HR Evolution spectrometer with a laser wavelength of 532 nm. X-ray photoelectron spectra were recorded using a Thermo Scientific K-Alpha spectrometer operated at  $5 \times 10^{-7}$  mBar pressure with an Al K $\alpha$  excitation source ( $h\nu = 1486.6$  eV). Survey spectra were recorded at 150 eV pass energy in 1 eV steps, with high-resolution spectra recorded at 50 eV pass energy in 0.1 eV steps. XP spectra were energy referenced to the C 1s peak of adventitious carbon at 284.8 eV. Thermogravimetric analysis was performed using a Netzsch STA 449 F5 instrument, with samples placed in alumina crucibles and heated under flowing air at  $10$  °C.min<sup>-1</sup>. Scanning electron microscopy and energy dispersive spectroscopy were performed using a ZEISS Sigma 360 system. Inductively coupled plasma optical emission spectroscopy was performed using a NCS Plasma 3000 analyser to determine the silicon and metal impurity content of samples (digested using HNO<sub>3</sub>, HF, and HClO<sub>4</sub> in a digestion instrument).

**Table S1.** FJH parameters explored.

Precursors	Mass Ratio	Mass (mg)	Resistance ( $\Omega$ )	Voltage (V)	Times of flash	Regrinding	Mass after FJH (mg)
c-Si: CB	1:1	250	2.5	100	1		241
c-Si: CB	1:1	250	2.5	115	1		240
c-Si: CB	1:1	250	2.5	130	1		233
c-Si: CB	1:1	250	2.5	145	1		232
c-Si: CB	1:1	250	2.5	160	1		224
c-Si: CB	1:1	250	2.5	130	2		232
c-Si: CB	1:1	250	2.5	130	2	√	219
c-Si: CB	1:1	250	2.5	130	6		230
c-Si: CB	1:1	250	2.5	130	6	√	217
c-Si: CB	1:1	250	2.5	130	10		226
c-Si: CB	1:1	250	2.5	130	10	√	211
c-Si: CB	2:1	250	2.5	130	1		234
c-Si: CB	1:2	250	2.5	130	1		230
c-Si: CB	1:4	250	2.5	130	1		231

**Text S2: Numerical simulation**

Temperature distribution simulations were conducted using the Joule heat mode in COMSOL Multiphysics finite element software. Geometric parameters: quartz tube length (25 cm); quartz tube inner diameter (0.8 cm); quartz tube outer diameter (1.4 cm); electrode diameter (0.8 cm); electrode length (0.5 cm); material diameter (0.8 cm); and material length (1.5 cm). Boundary conditions: input voltage (130 V), ground (0 V).

**Text S3. Metal removal efficiency and silicon-based yield**

The mass of sample used for FJH was  $m_s$ , the concentration of precious metals in sample was measured as  $c_s$ , the mass of product after FJH was  $m_p$ , the concentration of precious metals in product after FJH was measured as  $c_p$ , the mass of SiC in the flash heated product is  $m_p(\text{SiC})$ , the Si concentration in sample was measured as  $c_s(\text{Si})$ . The data used in this equation were obtained from ICP and TG analyses.

The metal removal efficiency was calculated using equation S1.

$$R = 1 - \frac{c_p \times m_p}{c_s \times m_s} \quad (\text{S1})$$

The metal silicon-based yield was calculated using equation S2. The optimal silicon-based yield of the sample (1:1 mass ratio of c-Si:CB) treated via regrind-assisted repeated FJH at 130 V is found to be ~95%. After calcination, the purity of SiC is approximately 96-98%, attributable to the presence of minor impurities (such as residual silicon, metals, and oxides, etc.).

$$Y = \frac{m_p(\text{SiC}) \times 0.7}{c_s(\text{Si}) \times m_s} \quad (\text{S2})$$

#### **Text S4: Calculation of energy consumption**

Energy consumption was calculated using equation S3.

$$E = \frac{(U_1^2 - U_2^2) \times C \times N}{2 \times M} \quad (\text{S3})$$

where  $E$  is energy per gram ( $\text{kJ} \cdot \text{g}^{-1}$ ),  $U_1$  and  $U_2$  are the voltages before and after flash Joule heating, respectively,  $C$  is the capacitance ( $C = 90 \text{ mF}$ ),  $N$  is the times of flash, and  $M$  is the mass per batch. For typical experiments where  $U_1 = 130 \text{ V}$ ,  $U_2 = 0 \text{ V}$ ,  $N=1$ , and  $M = 0.25 \text{ g}$ , the energy consumption  $E=3.04 \text{ kJ} \cdot \text{g}^{-1} = 8.45 \times 10^{-1} \text{ kWh} \cdot \text{kg}^{-1}$ . The yield of silicon carbide was increased using  $U_1 = 130 \text{ V}$ ,  $U_2 = 0 \text{ V}$ ,  $N=10$ , and  $M = 0.25 \text{ g}$ , for which the energy consumption  $E=30.42 \text{ kJ} \cdot \text{g}^{-1} = 8.45 \text{ kWh} \cdot \text{kg}^{-1}$ .

#### **Text S5: Electrochemical measurements**

N-methyl pyrrolidone (99.9 %) was used as the solvent for the assembly of half-cells. The FJH product, acetylene black (99.9 %), and polyvinylidene difluoride (99.5 %) were ground in a mortar and mixed in a mass ratio of 7:2:1 and coated onto a copper foil, vacuum-dried at  $80 \text{ }^\circ\text{C}$  for 12 h, and then cut into 14 mm diameter electrode discs. A lithium sheet served as the counter electrode, with a Celgard 2400 polymer membrane used as the separator. The electrolyte comprised  $\text{LiPF}_6$  (1M) dissolved in a 1:1 (vol%) mixture of ethylene carbonate and dimethyl carbonate. The components were assembled into button cells in an Ar filled glove box and tested after 12 h stabilization at  $25 \text{ }^\circ\text{C}$ . Stability tests were conducted on the cells at a current density of  $0.05 \text{ A g}^{-1}$  between 0.01 V to 3 V. Cycling tests were performed at current densities of 0.025, 0.05, 0.1, 0.2, 0.5, 1, and  $2 \text{ A g}^{-1}$ . A Neware CT-3008 electrochemical workstation was used to perform cyclic voltammetry with a scan rate of  $0.1 \text{ mV s}^{-1}$  between 0.01 to 3 V, and electrochemical impedance spectroscopy for frequencies spanning 0.01 Hz to 1 MHz. The supplier of the battery assembly process consumables is Guangdong Canrd New Energy Technology Co., Ltd.

#### **Text S6: Life cycle assessment**

##### **6.1 Goal and scope definition**

This study aimed to analyze and compare the environmental impacts of common recycling processes for used crystalline silicon photovoltaic cells, including chemical recycling, thermal recycling, and FJH recycling for producing silicon carbide. Specifically, energy consumption and greenhouse gas emissions at different stages of each recycling process were quantified and compared to assess whether FJH recycling offered superior environmental benefits.

##### **6.2 Recycling process and system boundaries definition**

Recycling of waste c-Si PV modules involves multiple steps, and hence each of the three recycling processes were simplified as flowcharts to facilitate direct comparison (**Figure 5a**). Data were obtained from relevant literature and SimaPro software and used to derive metrics for the recycling and processing of one ton of used

crystalline silicon PV modules. The system boundary was defined by the input of raw materials (waste c-Si PV modules) and the output of recycled products and waste.

### **6.3 Recycling process steps**

Transportation: transport of the waste PV modules to a waste treatment plant, assuming a transport distance of 150 km. Pre-dismantling: aluminium frames, junction boxes and wires are mechanically dismantled from the modules, the copper metal is further separated and the remaining plastics are incinerated to recover energy.

#### *Chemical recycling*

1. Layering: remaining components are immersed in a 99.5 % toluene solution, heated to dissolve most of the EVA and achieve component separation; short-term thermal decomposition is then applied to extract valuable components, mainly silicon and various metals. Toluene solution recovery assumed 97.3 %. Separated backsheets, EVA and other plastic waste are incinerated to recover some of the energy.
2. Chemical etching: the Ag and Cu metals in the remaining material were dissolved using 60% nitric acid, the anti-reflection coating and p-n junction were removed by mechanical treatment, and finally the residual Al metal was dissolved by 45% potassium hydroxide (KOH).
3. Metal extraction: collect the solution generated in the preceding step and recover Ag and Cu metals from it via electrolysis.
4. Waste treatment: nitric acid-containing liquid waste generated during the recycling process is neutralized with calcium hydroxide (Ca(OH)<sub>2</sub>) solution, potassium hydroxide (KOH)-containing liquid waste is neutralized with sulfuric acid solution, and other solid wastes are disposed of via sanitary landfilling.

#### *Thermal recycling*

1. Combustion: pre-disassembled modules are placed in a furnace for high-temperature treatment to remove the EVA and backsheets while recovering some of the energy.
2. Sieving and acid leaching: the burnt ash is sieved to separate some of the Al metal and then acid leached using 60% nitric acid to dissolve the other metals.
3. Metal extraction: after acid leaching is completed, the solution is filtered and the Ag and Cu metals are recovered from it by electrolysis.
4. Waste treatment: nitric acid-containing liquid waste generated during the recycling process is neutralized with calcium hydroxide (Ca(OH)<sub>2</sub>) solution, and other solid wastes are disposed of via sanitary landfilling.

#### *FJH recycling*

1. Separation and screening: glass and backsheet separated by mechanical processing and heat treatment, and residual c-silicon fragments collected. Separated backsheets, EVA and other plastic waste are incinerated to recover some of the energy.
2. Mixing: c-Si fragments crushed, ground, and mixed with conductive carbon black (or other source of waste carbon) in desired proportion.
3. Flash Joule heating: From the perspectives of operational efficiency and economic feasibility, the single flash heating was selected in the recycling process for the synthesis of silicon carbide.
4. Calcination: the product of silicon carbide produced by Joule heating is calcined to remove excess carbon and achieve purification of silicon carbide.

The life cycle inventory of each processing stage is detailed in **Table S2**.

**Table S2.** Life cycle inventory

<b>Impact Category</b>	<b>Energy consumption (MJ)</b>	<b>GHG emission (kg)</b>	<b>Water consumption (kg)</b>
Transportation and pre-dismantling	181.2	42.18	0
Layering	13100	4101	0
Chemical etching	524	155	560
Metal extraction (CR)	146.1	33.5	
Metal extraction (TR)	126.7	32.2	310
Sieving and acid leaching	71.5	21.2	
Combustion	6410	2093	0
Separation and screening	2090	802	0
Mixing	20.8	6.14	0
Flash Joule heating	302	129.5	0
Calcination	883	418.67	0

#### 6.4 Life cycle impact assessment (LCIA)

LCIA modelling was performed using SimaPro software to determine energy consumption (**Table S3**), GHG emissions (**Table S4**), materials consumption (**Table S5**), overall process cost (**Table S6**), product value (**Table S7**) and comparison of different reaction scales (**Table S8**). Uncertainties arise from variations in data sources, scale-up of the FJH recycling process (data in this study were obtained at milligram-scale), and market prices.

**Table S3.** Cumulative energy consumption for different recycling processes

<b>Recycling process</b>	<b>Chemical recycling (MJ)</b>	<b>Thermal recycling (MJ)</b>	<b>FJH recycling (MJ)</b>
Transportation and pre-dismantling	181.2	181.2	181.2
Layering	13100	0	0
Chemical etching	524	0	0
Metal extraction	146.1	126.7	0
Sieving and acid leaching	0	71.5	0
Combustion	0	6410	0
Separation and screening	0	0	2090
Mixing	0	0	20.8
Flash Joule heating	0	0	302
Calcination	0	0	883
<b>Total</b>	<b>13951.3</b>	<b>6789.4</b>	<b>3477</b>

**Table S4.** Cumulative GHG emissions for different recycling processes.

Recycling process	Chemical recycling	Thermal recycling	FJH recycling
	(kg)	(kg)	(kg)
Transportation and pre-dismantling	42.18	42.18	42.18
Layering	4101	0	0
Chemical etching	155	0	0
Metal extraction	33.5	32.2	0
Sieving and acid leaching	0	21.2	0
Combustion	0	2093	0
Separation and screening	0	0	802
Mixing	0	0	6.14
Flash Joule heating	0	0	129.5
Calcination	0	0	418.67
<b>Total</b>	<b>4331.7</b>	<b>2188.6</b>	<b>1398.5</b>

**Table S5.** Materials consumption for different recycling processes.

Material	Chemical recycling	Thermal recycling	FJH recycling
	(kg)	(kg)	(kg)
Water	560	310	0
Toluene	34.27	0	0
Nitric acid	60	7.08	0
Potassium hydroxide	63.7	0	0
Calcium hydroxide	25.3	36.5	0
Sulfuric acid	27.7	0	0

**Table S6.** Overall cost of different recycling processes.

Recycling process	Chemical recycling	Thermal recycling	FJH recycling
	(CNY)	(CNY)	(CNY)
Transportation and pre-dismantling	39.20	39.20	39.20
Layering	2388.95	0	0
Chemical etching	425.90	0	0
Metal extraction	62.87	123.58	0
Sieving and acid leaching	0	25.09	0
Combustion	0	1068.33	0
Separation and screening	0	0	348.33
Mixing	0	0	3.47
Flash Joule heating	0	0	50.33
Calcination	0	0	147.17
<b>Total</b>	<b>2916.92</b>	<b>1256.21</b>	<b>588.50</b>

Assuming all energy consumed is sourced from electricity, with an industrial electricity price of 0.6 CNY/kWh. The prices of water, toluene, nitric

acid, potassium hydroxide, sulfuric acid and calcium hydroxide are taken as 2.5 CNY/ton, 6,000 CNY/ton, 1,800 CNY/ton, 3,600 CNY/ton, 700 CNY/ton and 750 CNY/ton, respectively, and subject to fluctuations in actual market prices.

**Table S7.** Products and value for different recycling processes.

Products	Chemical recycling	Thermal recycling	FJH recycling
	(kg)	(kg)	(kg)
Waste glass	638	654	686
Aluminum	180	182.6	180
Silicon	21.3	34.7	0
Copper	6.2	4.4	3.3
Silver	0.6	0.5	0
Silicon carbide	0	0	46.9

Recycling values of glass, aluminum, silicon, copper, silver, and silicon carbide are assumed to be 0.6 CNY/kg, 16 CNY/kg, 11 CNY/kg, 65 CNY/kg, 6,000 CNY/kg, and 6 CNY/kg, respectively, and subject to fluctuations in actual market prices. Recycling 1 tonne of waste PV modules, the total value of the products recovered by CR, TR, and FJH is 7500.1 CNY, 6981.7 CNY, and 3787.5 CNY, respectively; meanwhile, the energy recovered during the CR, TR, and FJH processes is 420.86 MJ, 1835.46 MJ, and 435.33 MJ, respectively.

**Table S8.** Comparison of different reaction scales

Scale of reaction	250mg	10g	100g
Energy consumption of FJH (MJ)	302	402	1790
GHG emission from FJH (kg)	129.5	159.1	569.1
Total energy consumption (MJ)	3477	3577	4965
Total greenhouse gas emissions (kg)	1398.49	1428.09	1838.09
Total cost (CNY)	588.50	605.17	836.50



**Figure S1.** Photographs of (a) waste c-Si PV cell fragments, and (b) milled c-Si PV cell powder. Using Dong Yi multi-function pulverizer 800Y, rated power: 1400W, motor speed: 3400r/min, pulverizing time: 5 min. (c) Powder X-ray diffractogram of milled c-Si PV cell powder alongside reference pattern for Si (PDF: 075-0589).

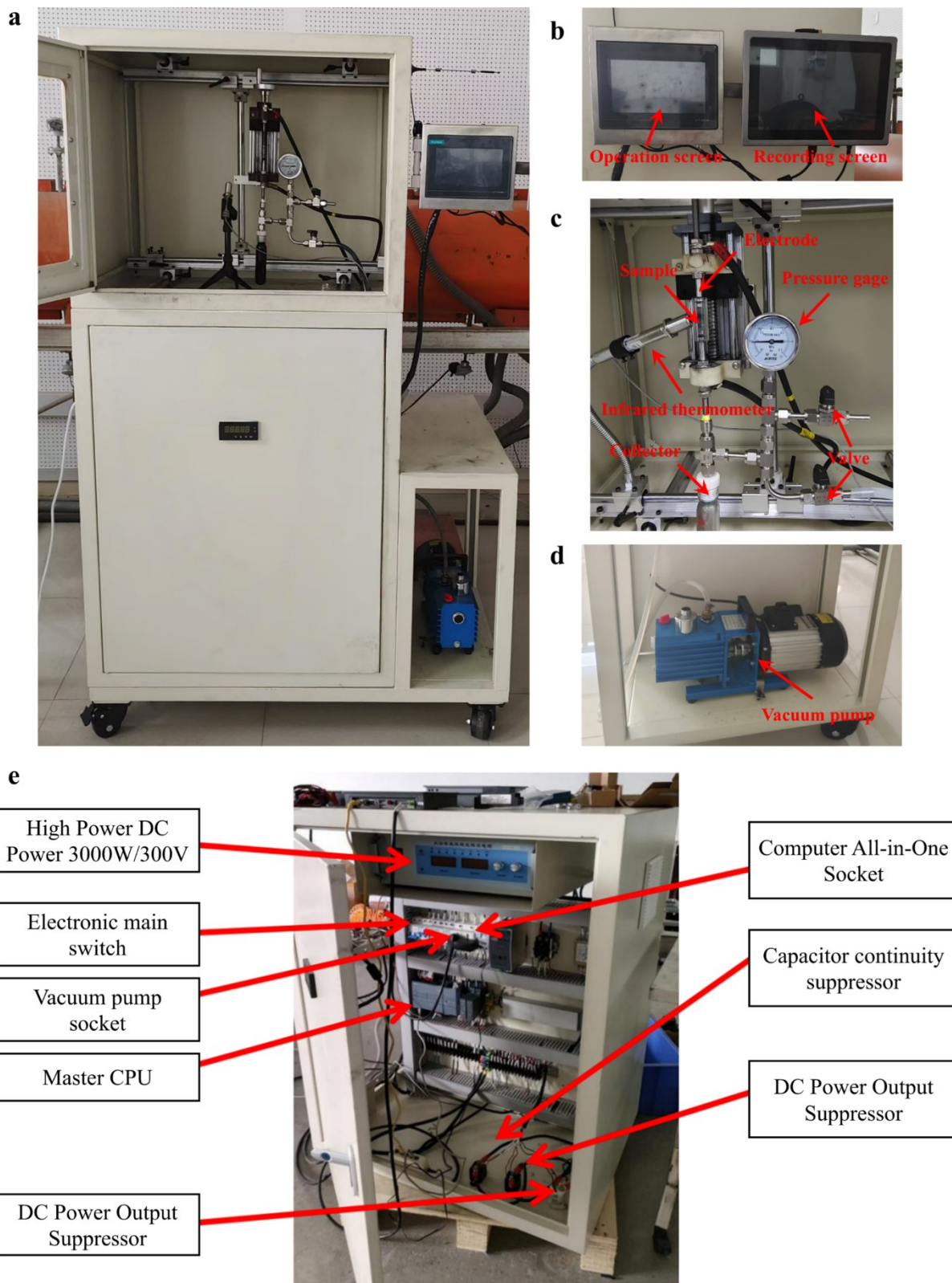


**Figure S2.** Photographs of FJH reactor and main components. (a) Entire reactor system. (b) Operating screen and data acquisition device. (c) Flash reaction section. (d) Vacuum pump. (e) Internal components.

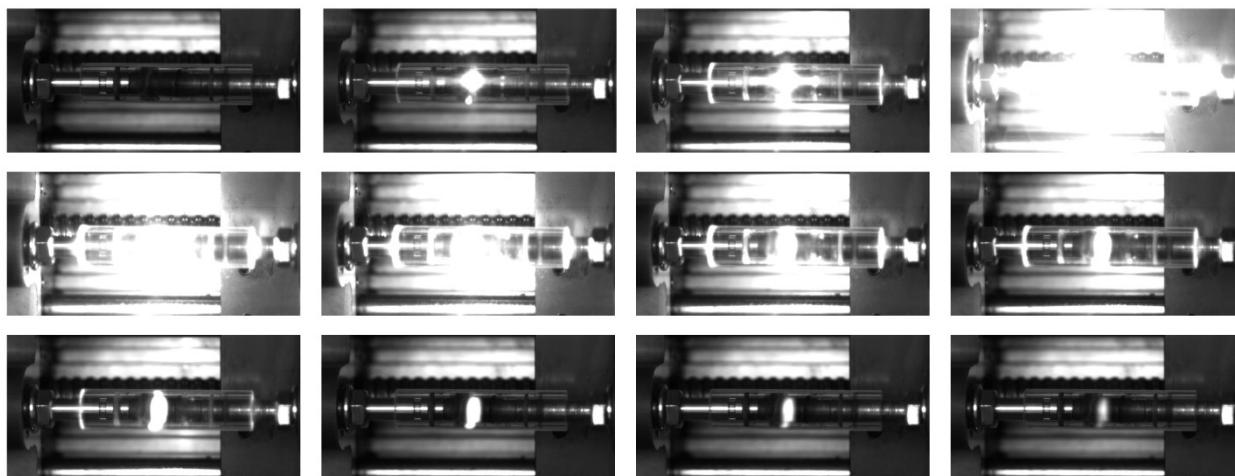


**Figure S3** High-speed photographs of the FJH process with an input voltage of 130V and 1:1 mass ratio of c-Si powder : CB.

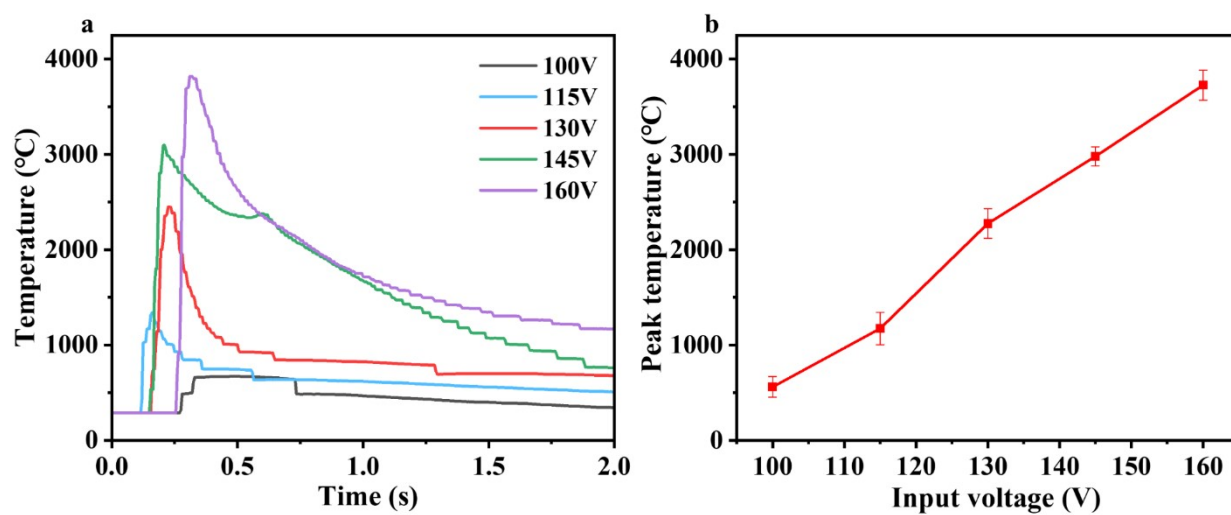


**Figure S4** (a) Relationship between sample temperature and input voltage. (b) Peak temperature during a single flash heating as a function of input voltage.

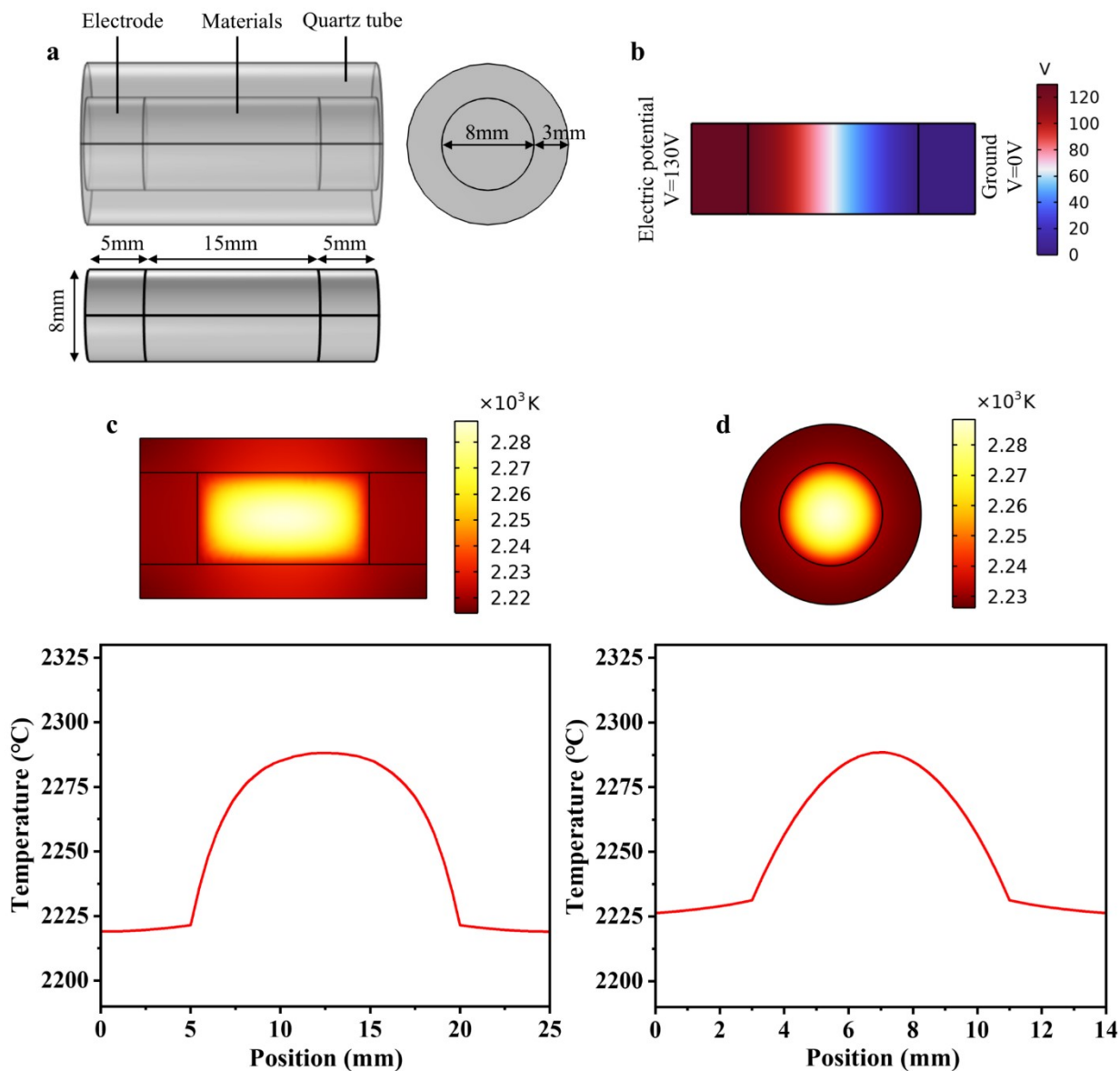


**Figure S5.** Temperature and potential simulation of FJH using COMSOL Multiphysics finite element software. (a) Geometric parameters. (b) Boundary conditions. (c) Temperature distribution and profile of the sample along the radial direction. (d) Temperature distribution and profile of the sample along the longitudinal direction. Flash Joule heating (FJH) is uniform in the longitudinal and the radial directions.

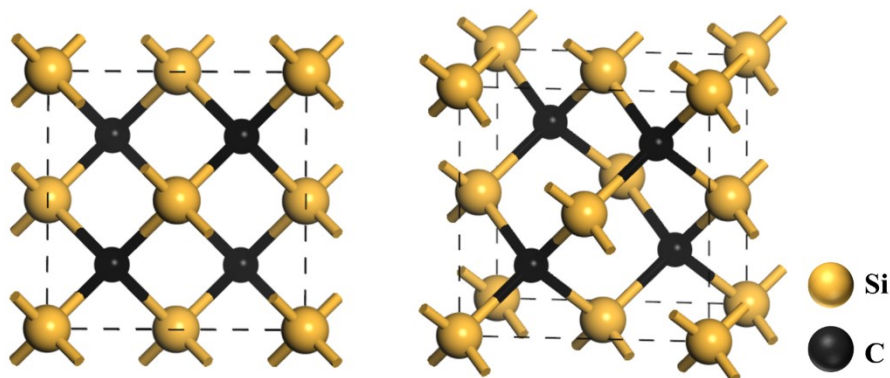


**Figure S6.** Cubic crystal structure of 3C-SiC wherein each silicon (Si) atom forms covalent bonds with four surrounding carbon (C) atoms, and each C is similarly bonded to four Si.

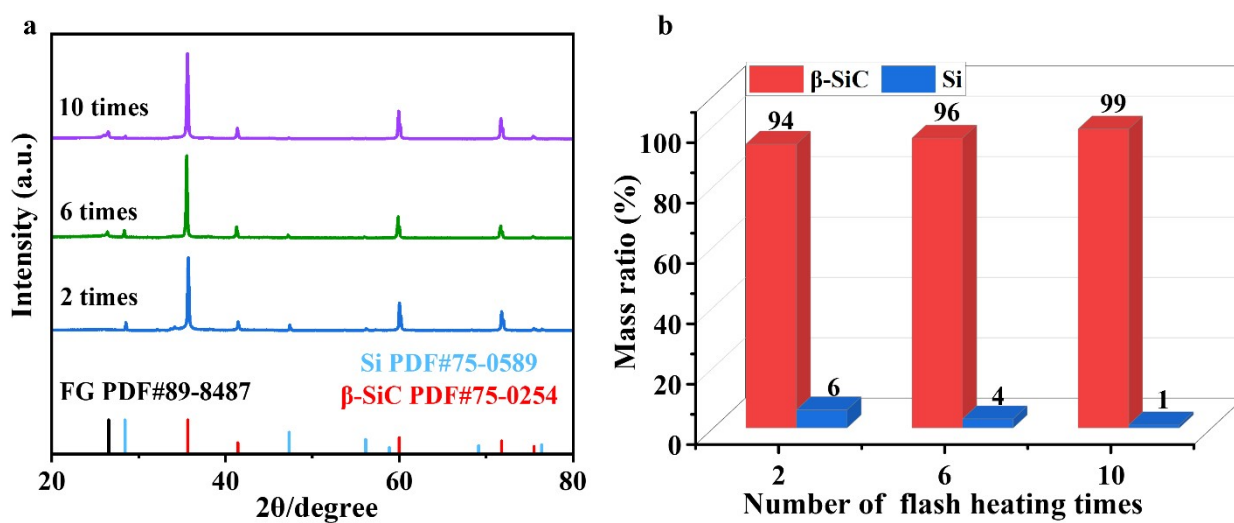


**Figure S7.** Impact of repeated FJH (and regrinding) cycles. (a) Powder X-ray diffractograms of products as a function of FJH cycles for a 1:1 mass ratio of c-Si powder : CB at 130 V. (b) Mass ratio of β-SiC to residual Si in products as a function of FJH cycles at 130 V.

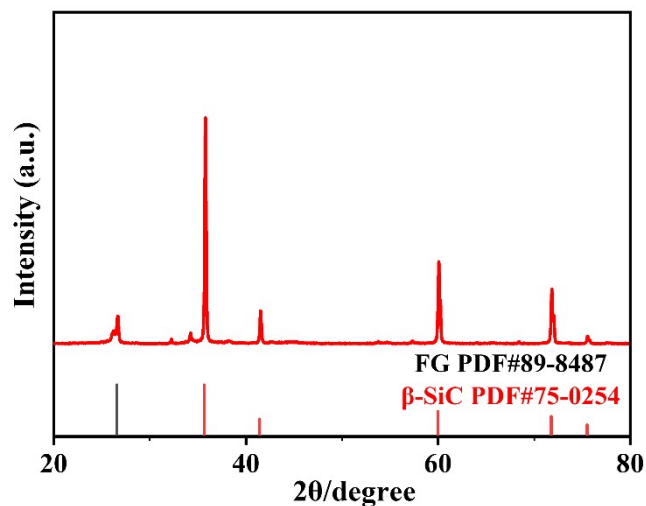


**Figure S8.** Powder X-ray diffractograms of product after continuous 20 FJH (and regrinding) cycles at 145 V for a 1:1 mass ratio of c-Si powder : CB.

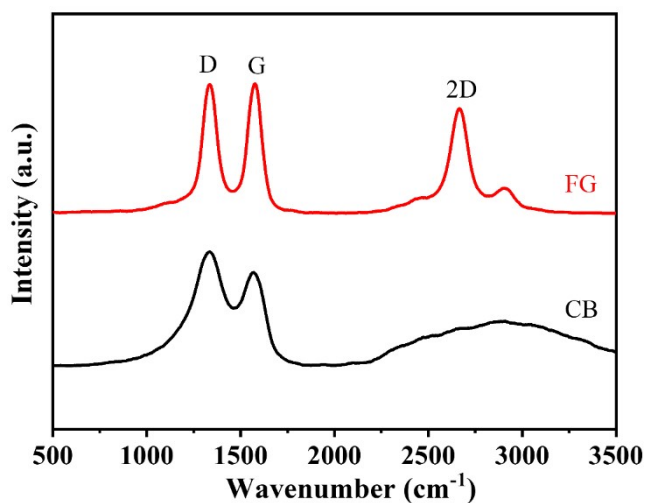


**Figure S9.** Raman spectra of CB before and after a single FJH cycle at 130 V.

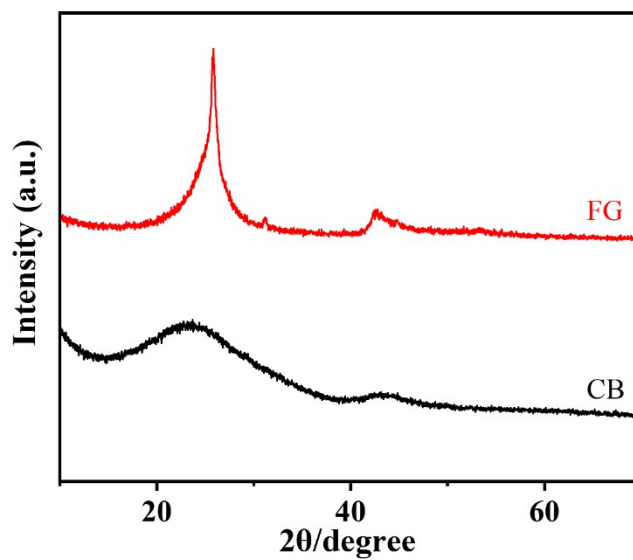


**Figure S10.** X-ray diffractograms of CB before and after a single FJH cycle at 130 V.

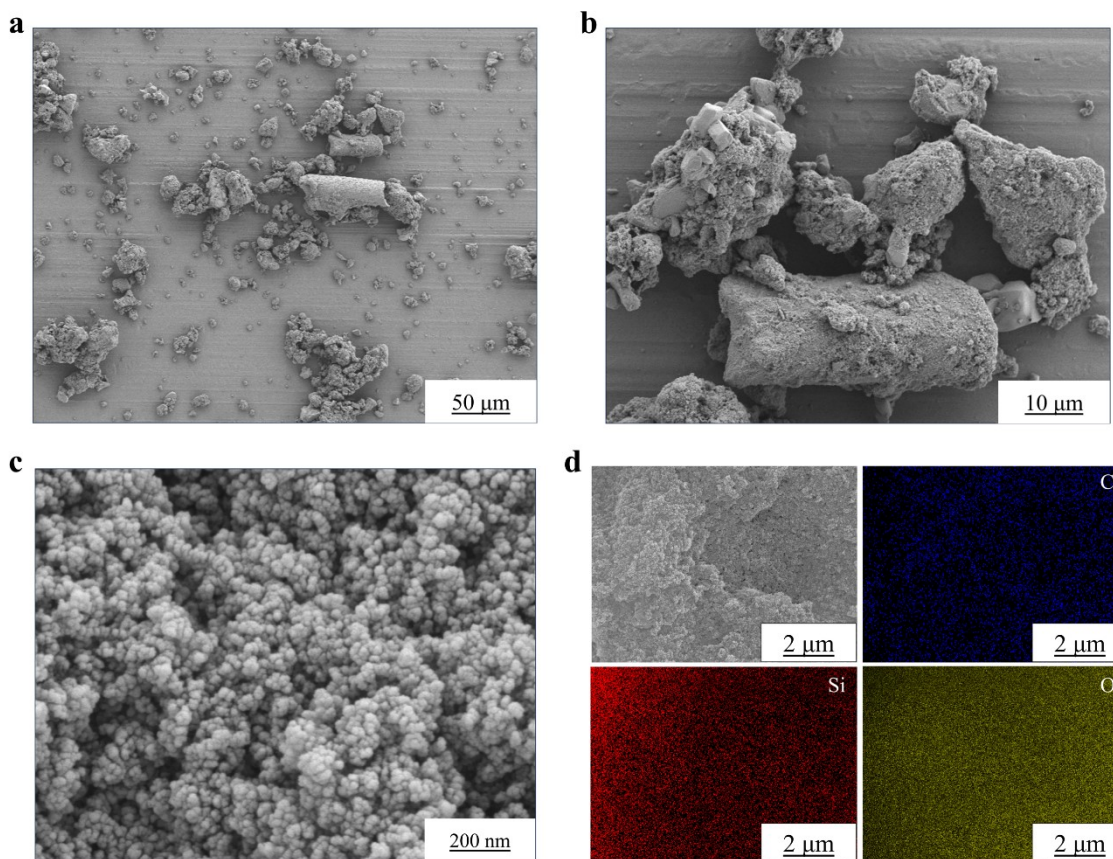


**Figure S11.** (a, b, c) SEM images, and (d) EDS elemental mapping of 10 cycles FJH product for a 1:1 mass ratio of c-Si powder : CB and 130 V.

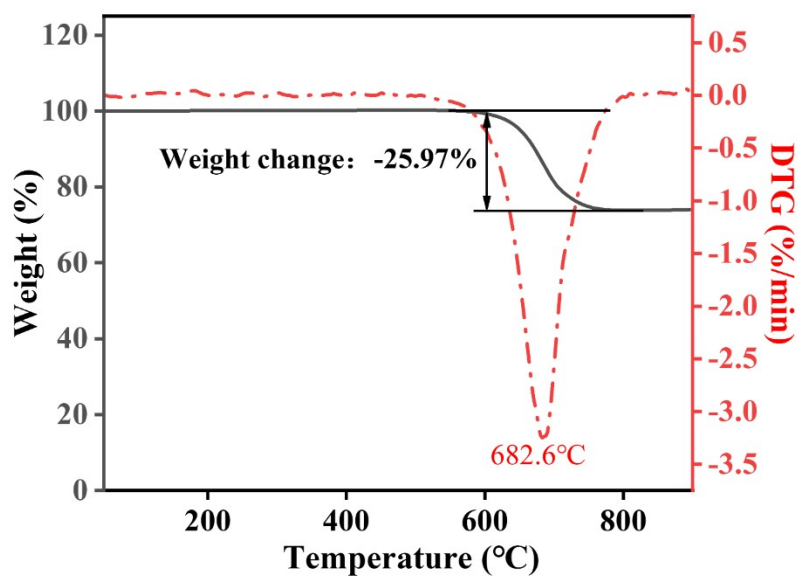


**Figure S12.** Thermogravimetric profiles of the FJH product in flowing air ( $50 \text{ mL min}^{-1}$ ) resulting from a 1:1 mass ratio of c-Si powder : CB. The heating rate was  $10 \text{ }^\circ\text{C}\cdot\text{min}^{-1}$ . Oxidation of residual free carbon commenced at  $\sim 567 \text{ }^\circ\text{C}$  and was complete by  $800 \text{ }^\circ\text{C}$  (total mass loss of 26 %). Continued heating to  $900^\circ\text{C}$ , 0.2% mass increase attributed to oxidation of SiC or residual impurities.

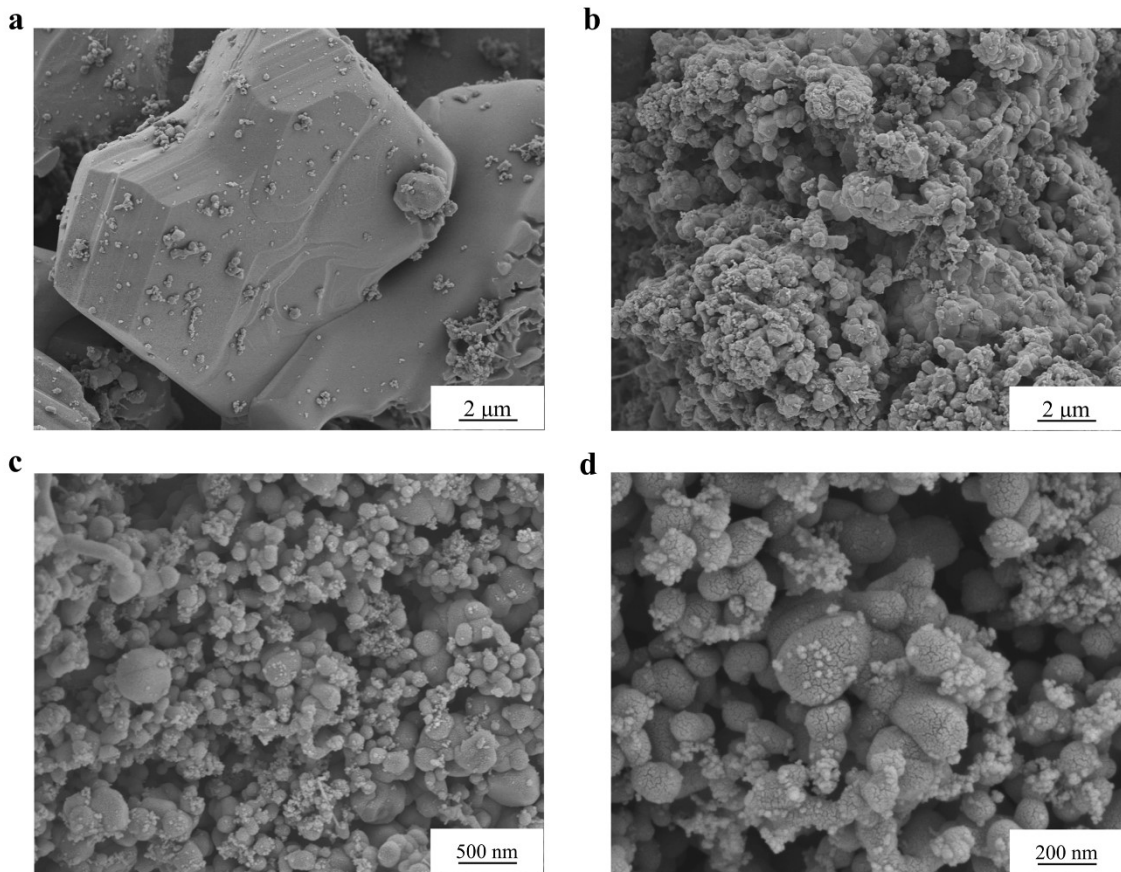


**Figure S13.** SEM images of 10 cycles FJH product after subsequent calcination in air at 700 °C for a 1:1 mass ratio of c-Si powder : CB at 130 V. (a) polygonal prismatic crystals spanning 1-30 μm, and (b,c,d) granular agglomerates formed from individual sub-particles spanning 100-400 nm.

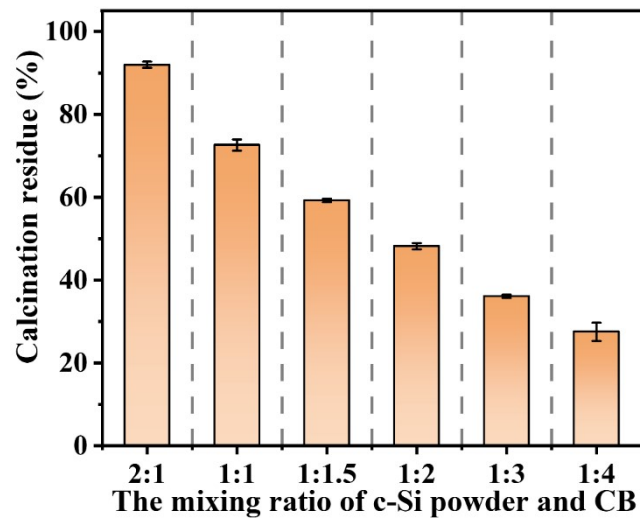


**Figure S14.** Residual mass of 10 cycles FJH product after subsequent calcination in air at 700 °C as a function of c-Si powder : CB mass ratio.

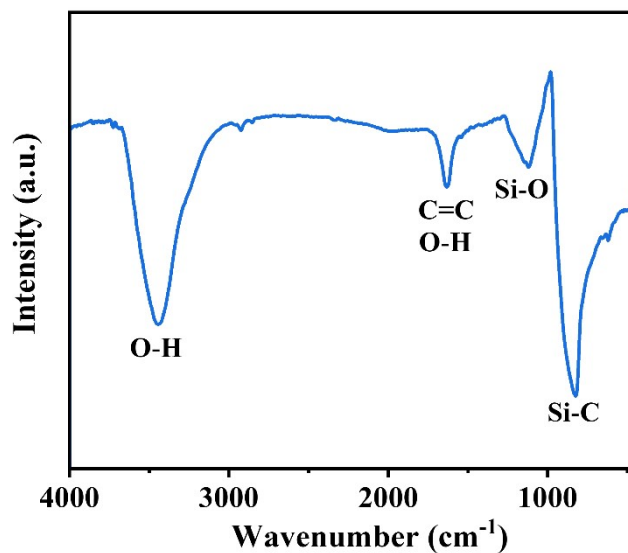


**Figure S15.** FT-IR spectra of 10 cycles FJH product after subsequent calcination in air at 700 °C for a 1:1 mass ratio of c-Si powder : CB at 130 V.

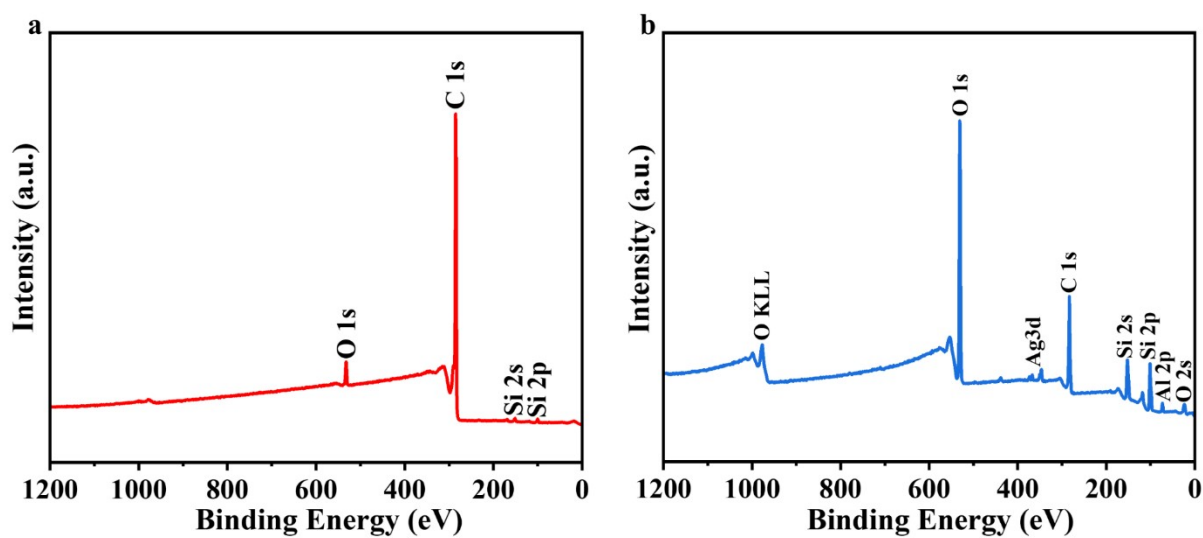


**Figure S16.** Survey XPS spectrum of 10 cycles FJH product at 130 V (a) before and (b) after calcination at 700 °C for 20 min.

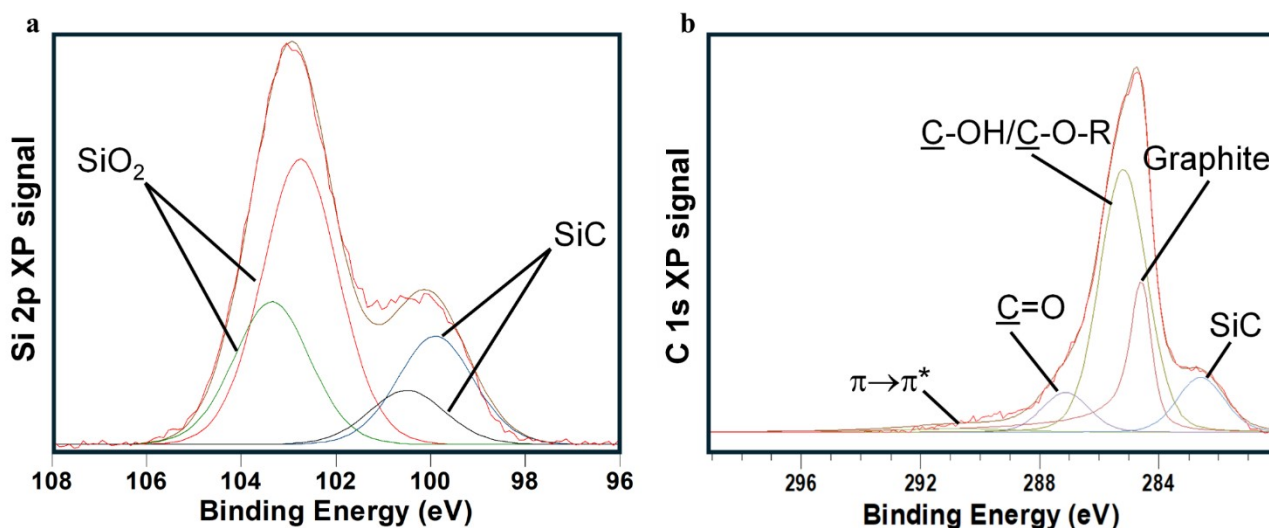


Figure S17. (a) Si 2p and (b) C 1s XP spectra of 10 cycles FJH product at 130 V after calcination at 700 °C for 20 min.

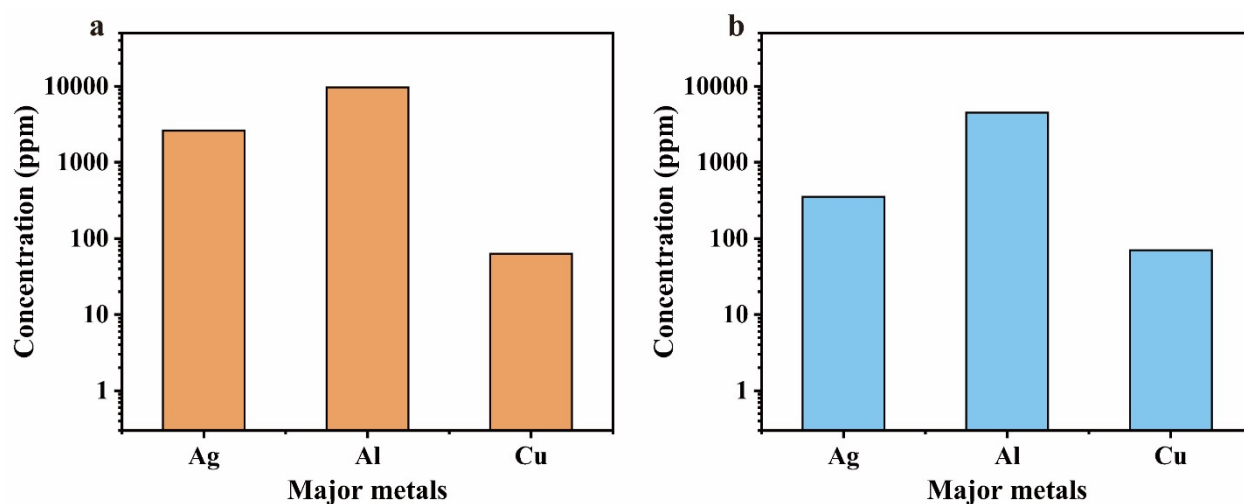


Figure S18. Concentration of trace metals in the c-Si/CB mixture (a) before and (b) after 10 cycles FJH at 130 V without calcination.

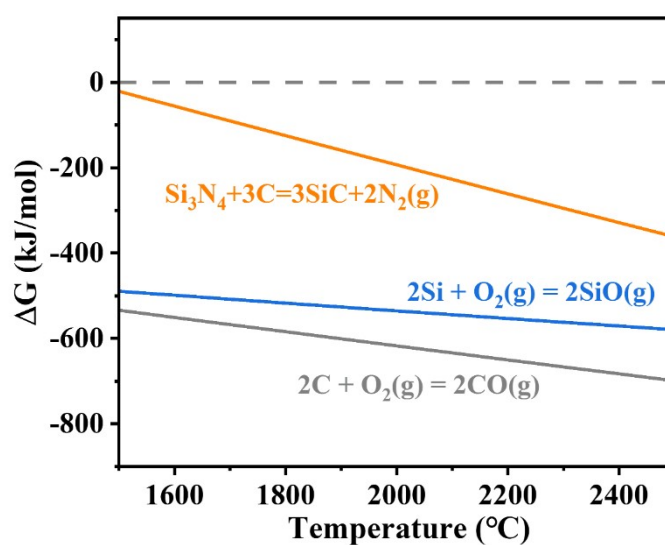
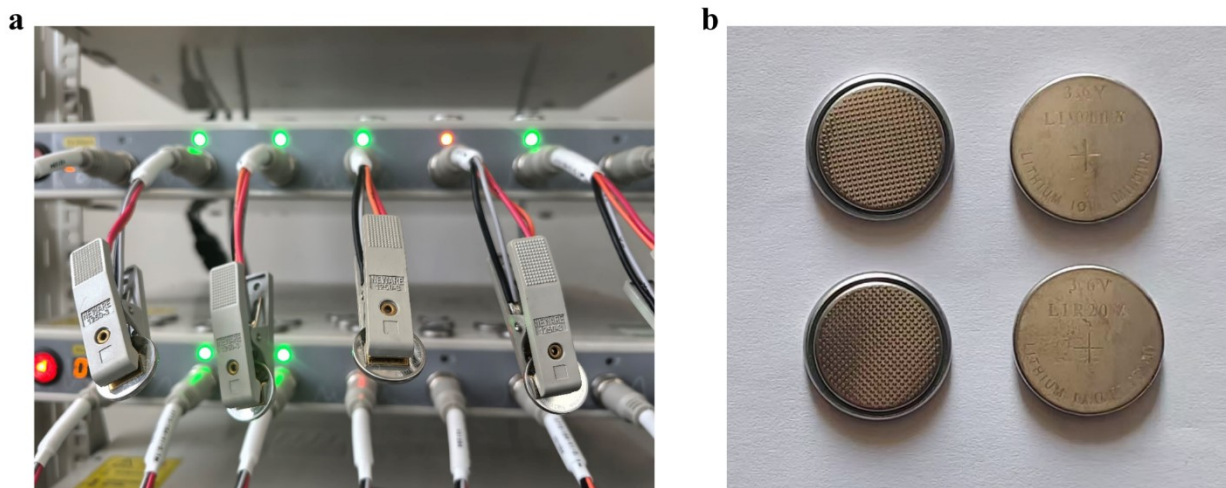
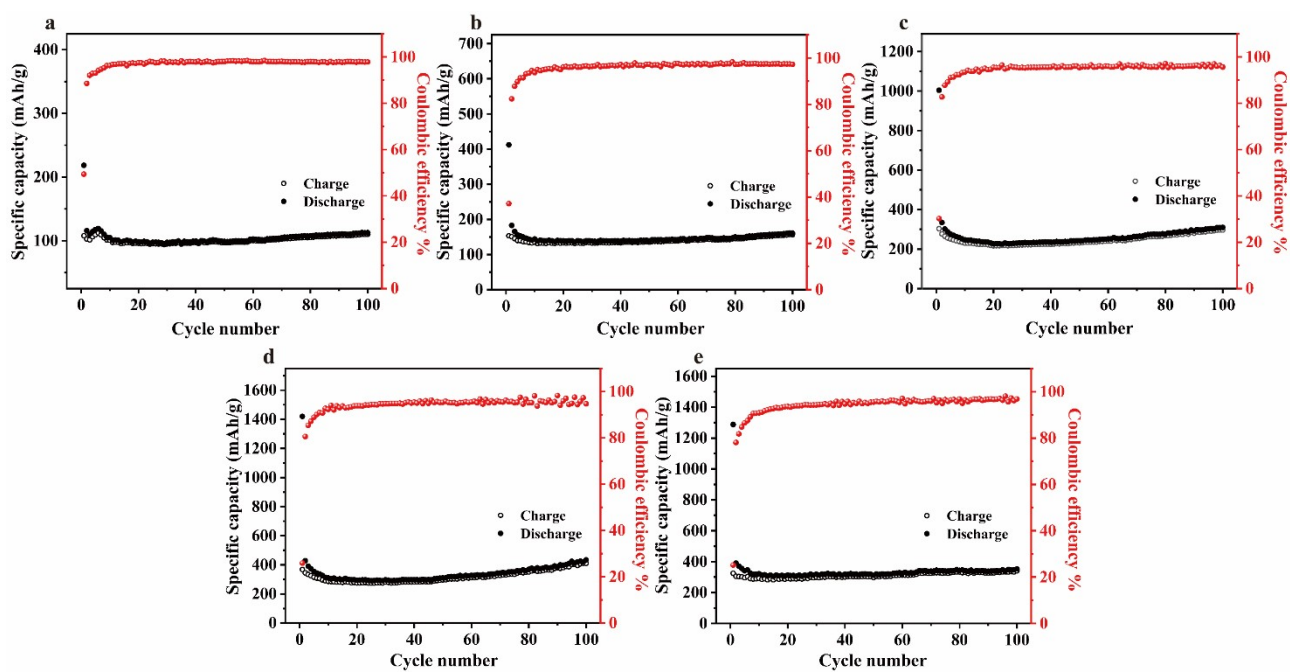


Figure S19. Gibbs free energy changes versus temperature for possible reactions during FJH; dashed line indicates  $\Delta G = 0$ .



**Figure S20.** Photographs of (a) electrochemical testing of silicon carbide anodes, and (b) close-up silicon carbide anode cell.



**Figure S21.** Specific capacity and cycling stability of different wt% SiC anodes produced by blending with different amounts of FG: (a) 99 % (calcined to remove FG); (b) 73 %; (c) 49 %; (d) 27 %; (e) SiC-free FG.

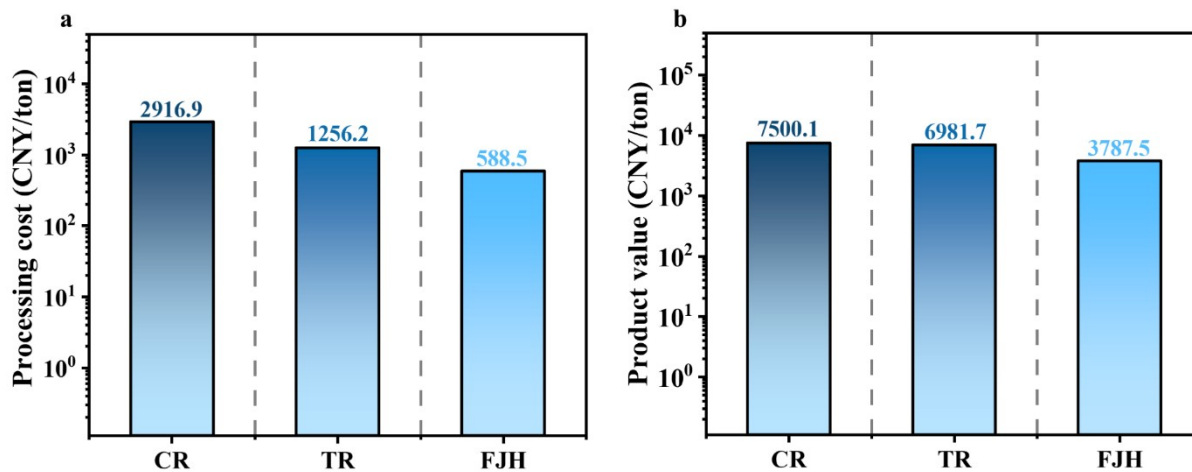


Figure S22. Comparison of (a) material and energy costs, and (b) cumulative product value.

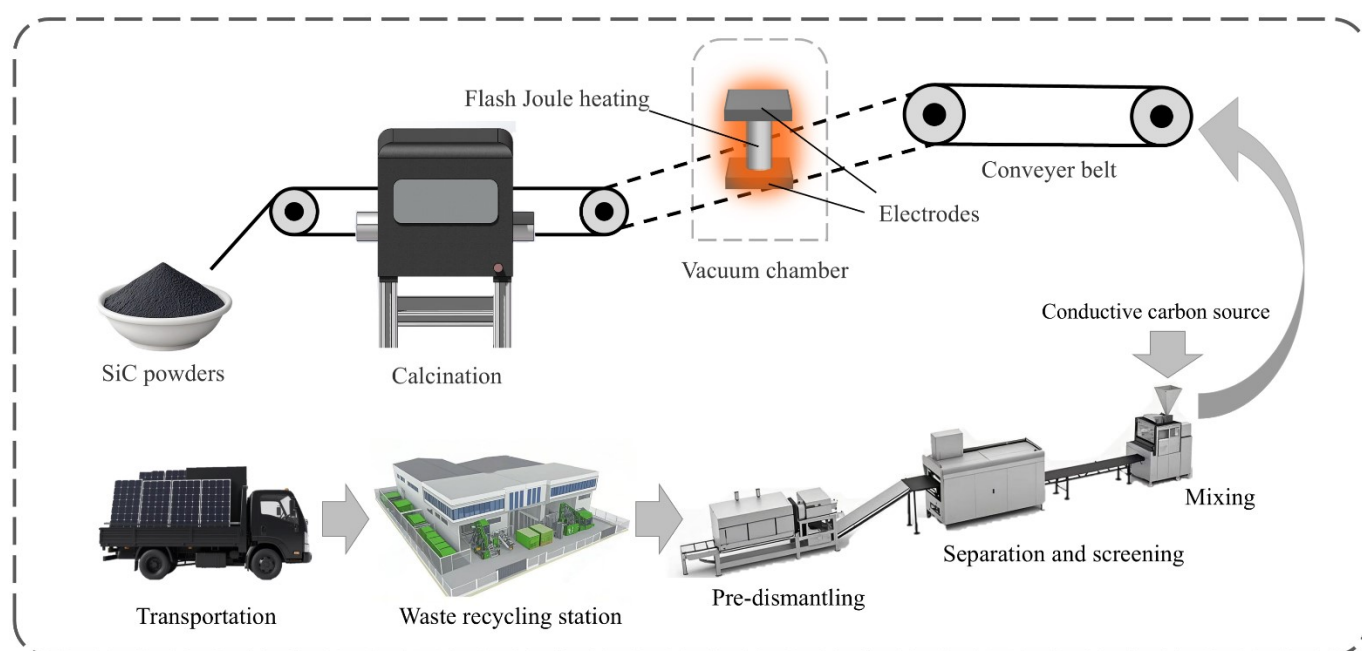


Figure S23. Schematic of large-scale continuous recycling of waste PV modules by flash Joule heating. Waste PV modules are transported to a recycling station, unloaded, and fed into a processing line. Waste undergoes pre-dismantling, separation, and screening, prior to mixing with a conductive carbon source. The resulting mixture is fed by a conveyor belt into a large capacity Joule heating stage, with the resulting FJH product passed through a furnace for calcination to produce the final silicon carbide powder.